Selective Oxygenation of 4,4′-Dimethylbiphenyl with Molecular Oxygen, Catalyzed by 9-Phenyl-10-methylacridinium Ion via Photoinduced Electron Transfer

Kyou Suga, Kei Ohkubo, and Shunichi Fukuzumi*

Department of Material and Life Science, Graduate School of Engineering, Osaka University, SORST, Japan Science and Technology Agency (JST), Suita, Osaka 565-0871, Japan

Received: June 26, 2005; In Final Form: September 6, 2005

Photooxygenation of 4,4′-dimethybiphenyl with oxygen occurs efficiently in the presence of 9-phenyl-10-methylacridinium perchlorate ($AcrPh^+ClO_4^-$) under visible light irradiation in O_2-saturated chloroform ($CHCl_3$) to yield 4-(4′-methylphenyl)benzaldehyde as a main oxygenated product. Prolonged photoirradiation afforded the further oxygenated product, 4,4′-diformylbiphenyl. The reactive radical intermediates involved in the photocatalytic cycle have successfully been detected by laser flash photolysis and electron spin resonance (ESR) measurements. The photocatalytic mechanism for the oxygenation of 4,4′-dimethybiphenyl via photoinduced electron transfer from 4,4′-dimethybiphenyl to the singlet excited state of $AcrPh^+$ is clarified based on the dependence of quantum yields on concentrations of substrates and the detected radical intermediates.

Introduction

The selective oxygenation of substrates is one of the most fundamental transformations in both laboratory and industrial synthetic chemistry because the corresponding carbonyl compounds serve as important and versatile intermediates for the synthesis of fine chemicals as pharmaceutical drugs and functional materials.[1] As an oxidant, oxygen is an ideal reagent because of its abundant ability and nontoxicity. The use of oxygen as an oxidant enables us to avoid the use of stoichiometric amounts of inorganic oxidants such as permanganate and dichromate.[2−4] Among a variety of oxygenation reactions, oxygenation of 4,4′-dimethylbiphenyl to yield 4-(4′-methylphenyl)benzaldehyde and 4,4′-diformylbiphenyl is particularly important because they are key chemical intermediates for production of fluorescent organic nanoparticles,[5] liquid crystals,[6] and muscular nicotinic receptor antagonists.[7] 4-(4′-Methylphenyl)benzaldehyde has so far been synthesized via bromination reaction of 4,4′-dimethylbiphenyl with *N*-bromosuccinimide and the subsequent formylation with hexamethylenetetramine.[5] 4,4′-Diformylbiphenyl was also synthesized by bromination of 4,4′-dimethylbiphenyl with hydrogen bromide and the subsequent formylation with $NaHCO_3$.[8,9] Thus, it is highly desired to develop one-step catalytic oxygenation of 4,4′-dimethylbiphenyl with molecular oxygen.

We have previously reported that selective photoinduced oxygenation of ring-substituted toluenes containing electron-donating or -withdrawing substituents with molecular oxygen is achieved by choosing appropriate photosensitizers that can act as photocatalysts via photoinduced electron transfer from ring-substituted toluenes to the excited state of sensitizers.[10] The judicious choice of photocatalysts and solvents is required depending on substrates to be selectively oxygenated by molecular oxygen.[10] However, the photocatalytic selective oxygenation of 4,4′-dimethylbiphenyl with molecular oxygen has yet to be achieved. The key step of the photocatalytic oxygenation reactions is the deprotonation of substrate radical cations in relatively nonpolar solvents such as chloroform ($CHCl_3$) to produce deprotonated radicals that can readily react with molecular oxygen.[10] Although the deprotonation dynamics of substituted toluenes has been examined in detail in an aqueous solution,[11,12] the deprotonation dynamics in aprotic or nonpolar solvents has yet to be reported.

We report herein the selective photocatalytic oxygenation reaction of 4,4′-dimethylbiphenyl with molecular oxygen to afford 4-(4′-methylphenyl)benzaldehyde and 4,4′-diformylbiphenyl using 9-phenyl-10-methylacridinium perchlorate ($AcrPh^+$-ClO_4^-) as an appropriate photocatalylst in $CHCl_3$, which was found to be the best solvent. The deprotonation step in $CHCl_3$ has successfully been monitored by laser flash photolysis measurements. The radical intermediates involved in the photocatalytic oxygenation reaction have also been detected by electron spin resonance (ESR) measurements under photoirradiation at low temperature. The quantum yield determination combined with the direct detection of the radical intermediates by laser flash photolysis and ESR measurements has enabled us to clarify the detailed photocatalytic mechanism.

Experimental Section

Materials. 4,4′-Dimethylbiphenyl was purchased from Tokyo Kasei Kogyo Co., Ltd. and was purified by successive chromatography on aluminum oxide (Merck, aluminum oxide 90 active neutral) with benzene as eluent.[13] 4,4′-Diformylbiphenyl was supplied from Ihara Chemical Co. 4-(4′-Methylphenyl)-benzaldehyde and chlorobenzene (C_6H_5Cl) were purchased from Tokyo Kasei Kogyo Co., Ltd. Acetonitrile (CH_3CN) and chloroform ($CHCl_3$) were purchased from Nacalai Tesque, Inc. Acetic acid was purchased from Wako Pure Chemical Ind., Ltd. 9-Phenyl-10-methylacridinium perchlorate ($AcrPh^+ClO_4^-$) was prepared by the reaction of 10-methylacridone with phenylmagnesium bromide in dichloromethane and then addition of sodium hydroxide for the hydrolysis and perchloric acid for the neutralization and purified by recrystallization from ethanol-diethyl ether. Potassium ferrioxalate used as an actinometer was

---

* To whom correspondence should be addressed. E-mail: fukuzumi@chem.eng.osaka-u.ac.jp.

10.1021/jp053465q CCC: $30.25

prepared according to the literature and purified by recrystallization from hot water.[14] Deuterated [$^2H_3$]acetonitrile (CD_3CN, 99.8%) and deuterated [^2H]chloroform ($CDCl_3$, 99.8%) were purchased from EURI SO-TOP, CEA, France and used as received. 9,10-Dihydro-10-methylacridine ($AcrH_2$) was prepared from 10-methylacridinium iodide ($AcrH^+I^-$) by reduction with $NaBH_4$ in methanol and purified by recrystallization from ethanol.[15,16] 4-(4′-Methylphenyl)benzyl alcohol was prepared by the reaction of 4-(4′-methylphenyl)benzaldehyde with the $LiAlH_4$ as follows. A solution of 4-(4′-methylphenyl)benzaldehyde (0.5 g, 2.6×10^{-3} mol) in absolute diethyl ether (1 cm^3) was added dropwise to a stirred solution of lithium aluminum hydride (0.03 g, 8.0×10^{-4} mol) in absolute diethyl ether (1 cm^3) under an argon atmosphere. After completion of the addition, the gray reaction mixture was refluxed for 30 min and was cooled to room temperature. It was then treated with diethyl ether (20 cm^3) and water (20 cm^3). The organic phase was separated, washed with water, and dried over anhydrous magnesium sulfated. Evaporation of the solvents in vacuo afforded a gray solid residue which upon chromatographic purification on silica gel with $CHCl_3$ as eluent afforded 4-(4′-methylphenyl)benzyl alcohol as a white powder (0.38 g, 75%).

Reaction Procedure. Typically, a $CDCl_3$ solution (0.6 cm^3) containing $AcrPh^+$ (4.0×10^{-3} M) and 4,4′-dimethylbiphenyl (3.0×10^{-2} M) in an NMR tube sealed with a rubber septum was saturated with oxygen by bubbling with oxygen through a stainless steel needle for 5 min. The solution was then irradiated with a mercury lamp through an acetophenone−methanol filter transmitting $\lambda > 300$ nm at room temperature. The products of the photooxidation of 4,4′-dimethylbiphenyl (3.0×10^{-2} M) with $AcrPh^+$ (4.0×10^{-3} M) in O_2-saturated $CDCl_3$ (0.6 cm^3) were determined by ^1H NMR. The ^1H NMR measurements were performed using a JEOL JMN-AL300 (300 MHz) NMR spectrometer. ^1H NMR (300 MHz, $CDCl_3$): 4-(4′-methylphenyl)benzaldehyde: δ 2.40 (s, 3H), 7.29 (d, 2H, $J = 7.9$ Hz), 7.55 (d, 2H, $J = 7.9$ Hz), 7.74 (d, 2H, $J = 8.4$ Hz), 7.94 (d, 2H, $J = 8.4$ Hz), 10.00 (s, 1H); 4,4′-diformylbiphenyl: δ 7.66 (d, 4H, $J = 8.3$ Hz), 8.15 (d, 4H, $J = 8.3$ Hz), 10.09 (s, 2H); 4-(4′-methylphenyl)benzyl hydroperoxide: δ 2.40 (s, 3H), 4.64 (s, 2H), 7.24−8.00 (m, 8H); 4-(4′-methylphenyl)benzyl alcohol: δ 2.40 (s, 3H), 4.74 (s, 2H), 7.22−7.57 (m, 8H); 4-(4′-formylphenyl)benzyl hydroperoxide: δ 2.40 (s, 3H), 4.66 (s, 2H), 7.27−8.23 (m, 8H), 10.12 (s, 1H); 4-(4′-formylphenyl)-benzyl alcohol: δ 2.40 (s, 3H), 4.78 (s, 2H), 7.27−8.23 (m, 8H), 10.06 (s, 1H). The amount of the hydroperoxide was determined by titration with iodide ion.[17] The aliquots of the product mixture in CH_3CN was treated with excess NaI, and the amount of I_3^- formed was determined by the UV−visible absorption spectrum ($\lambda_{max} = 361$ nm, $\epsilon_{max} = 2.5 \times 10^4$ M^{-1} cm^{-1})[18] using a Hewlett-Packard 8453 diode array spectrophotometer with a quartz cuvette (path length = 2 mm) at 298 K.

Determination of O_2 Concentrations in $CHCl_3$. A square quartz cuvette (10 mm id) was filled with a deaerated $CHCl_3$ solution (5.5 cm^3) containing 10-methyl-9,10-dihydroacridine ($AcrH_2$, 3.0×10^{-2} M) and acetic acid (1.6×10^{-3} M), and then air-saturated $CHCl_3$ (0.055 cm^3) was added. When the absorption band of $AcrH_2$ ($\lambda = 285$ nm) was irradiated with monochromatized light using a Shimazu spectrofluorophotometer (RF-5300PC), the absorption band due to $AcrH^+$ ($\lambda = 361$ nm, $\epsilon = 1.8 \times 10^4$ M^{-1} cm^{-1}) appeared, and the absorbance reached a limiting value after prolonged photoirradiation. Since $AcrH_2$ is oxidized by an equivalent amount of oxygen to produce $AcrH^+$ in the presence of an acid under photoirradiation,[19] the concentration of oxygen in air-saturated $CHCl_3$ was determined as 8.0×10^{-3} M from the limiting value of the absorbance and the ϵ value of $AcrH^+$ in $CHCl_3$. The O_2 concentration in the O_2-saturated $CHCl_3$ was estimated as 5-fold of that in air-saturated $CHCl_3$.[19]

Quantum Yield Determination. A standard actinometer (potassium ferrioxalate)[14] was used for the quantum yield determination of formation of 4-(4′-methylphenyl)benzaldehyde by the $AcrPh^+$-photosensitized oxygenation of 4,4′-dimethylbiphenyl with oxygen. A square quartz cuvette (10 mm id) which contained a $CHCl_3$, C_6H_5Cl, or CH_3CN solution (3.0 cm^3) of $AcrPh^+$ (3.7×10^{-4} M) and 4,4′-dimethylbiphenyl (1.0×10^{-2}−4.0×10^{-2} M) was irradiated with monochromatized light of $\lambda = 430$ nm from a Shimadzu RF-5300PC fluorescence spectrophotometer. Under the conditions of actinometry experiments, both the actinometer and $AcrPh^+$ absorbed essentially all the incident light. The light intensity of monochromatized light of $\lambda = 430$ nm was determined as 1.61×10^{-10} einstein s^{-1} with the slit width of 20 nm. The photochemical reaction was monitored using a Shimadzu UV-3100PC spectrophotometer. The quantum yields of the oxygenation reactions were determined from an increase in the yield of 4-(4′-methylphenyl)-benzaldehyde ($\lambda = 300$ nm, $\epsilon = 21\,000$ M^{-1} cm^{-1}). To avoid the contribution of light absorption of the products, only the initial rates were determined for determination of the quantum yields.

Fluorescence Quenching. Quenching experiments of the fluorescence of $AcrPh^+$ by 4,4′-dimethylbiphenyl were performed using a Shimadzu RF-5300PC fluorescence spectrophotometer with the excitation wavelength (363 nm in $CHCl_3$). The monitoring wavelength was that corresponding to the maximum of the emission band (508 nm in $CHCl_3$).[10] The solutions were deoxygenated by argon purging for 10 min prior to the measurements. Relative emission intensities were measured for solutions containing $AcrPh^+$ (5.0×10^{-6} M) and 4,4′-dimethylbiphenyl (0−1.5×10^{-2} M) in $CHCl_3$, C_6H_5Cl, and CH_3CN. There was no change in the shape, but there was a change in the intensity of the fluorescence spectrum by the addition of 4,4′-dimethylbiphenyl. The Stern−Volmer relationship (eq 1) was obtained for the ratio of the emission intensities

$$I_0/I = 1 + K_{SV}[D] \tag{1}$$

in the absence and presence of electron donor (I_0/I) and the concentrations of quenchers [D]. The fluorescence lifetimes τ of $AcrPh^+$ in the various solvents were determined by using a Photon Technology International GL-3300 with a Photon Technology International GL-302, nitrogen laser/pumped dye laser system (50 ps pulse duration), equipped with a four channel digital delay/pulse generator (Stanford Research System Inc. DG535) and a motor driver (Photon Technology International MD-5020). All samples were excited at 430 nm with a repetition rate of 10 Hz (pulse width 3−4 ns) using POPOP (Wako Pure Chemical Ind. Ltd., Japan) as a dye in toluene, and the fluorescence signal was analyzed after passing through a monochromator set at the peak emission of the corresponding sample. The observed quenching rate constants k_q ($= K_{SV}\tau^{-1}$) were obtained from the Stern−Volmer constants K_{SV} and the fluorescence lifetimes τ.

Electrochemical Measurements. The second harmonic ac voltammetry (SHACV)[20] measurements of 4,4′-dimethylbiphenyl were performed on a BAS 100B electrochemical analyzer in deaerated CH_3CN containing 0.10 M Bu_4NClO_4 as a supporting electrolyte at 298 K. The platinum working electrode (BAS) was polished with BAS polishing alumina suspension and rinsed with acetone before use. The counter electrode was a platinum wire (BAS). The measured potentials were recorded with respect to the Ag/AgNO$_3$ (0.01 M) reference electrode. The E_{ox} and E_{red} values (vs Ag/Ag$^+$) are converted to those vs SCE by adding 0.29 V.[21]

ESR Measurements. An O$_2$-saturated dichloromethane (CH$_2$Cl$_2$) solution of AcrPh$^+$ (4.0×10^{-3} M) and 4,4′-dimethylbiphenyl (1.0×10^{-1} M) was irradiated at 198 K with a high-pressure mercury lamp (USH-1005D) through a water filter focusing at the sample cell in the ESR cavity. The ESR spectra were taken on a JEOL JES-RE1XE and were recorded under nonsaturating microwave power conditions. The magnitude of the modulation was chosen to optimize the resolution and the signal-to-noise ratio (S/N) of the observed spectra. The g values were calibrated using an Mn^{2+} marker.

Laser Flash Photolysis. Nanosecond laser flash photolysis measurements of the AcrPh$^+$-photosensitized reactions of 4,4′-dimethylbiphenyl in the absence and presence of oxygen were performed as follows. An O$_2$-saturated or deaerated CHCl$_3$ solution containing 4,4′-dimethylbiphenyl (1.0×10^{-1} M) and AcrPh$^+$ (5.6×10^{-5} M) was excited by an Nd:YAG laser (Continuum, SLII-10, 4−6 ns fwhm) at $\lambda = 355$ nm with the power of 30 mJ per pulse. Transient absorption spectra were measured by using a continuous Xe-lamp (150 W) and an InGaAs-PIN photodiode (Hamamatsu 2949) as a probe light and a detector, respectively. The output from the photodiodes and a photomultiplier tube was recorded with a digitizing oscilloscope (Tektronix, TDS3032, 300 MHz). Femtosecond laser flash photolysis was conducted using a Clark-MXR 2010 laser system and an optical detection system provided by Ultrafast Systems (*Helios*). The source for the pump and probe pulses were derived from the fundamental output of Clark laser system (775 nm, 1 mJ/pulse and fwhm = 150 fs) at a repetition rate of 1 kHz. A second harmonic generator introduced in the path of the laser beam provided 387 nm laser pulses for excitation. 95% of the fundamental output of the laser (775 nm) was used to generate the second harmonic, while 5% of the deflected output was used for white light generation. Prior to generating the probe continuum, the laser pulse was fed to a delay line that provided an experimental time window of 1.6 ns with a maximum step resolution of 7 fs. The pump beam was attenuated at 5 μJ/pulse with a spot size of 2 mm diameter at the sample cell where it was merged with the white probe pulse in a close angle (<10°). The probe beam after passing through the 2 mm sample cell was focused on a 200 μm fiber optic cable which was connected to a CCD spectrograph (Ocean Optics, S2000-UV−vis) for recording the time-resolved spectra (425−800 nm). Typically, 5000 excitation pulses were averaged to obtain the transient spectrum at a set delay time. Kinetic traces at appropriate wavelengths were assembled from the time-resolved spectral data. All measurements were performed using fresh solutions in each laser excitation at 298 K.

Results and Discussions

Photocatalytic Oxygenation of Dimethylbiphenyl with Oxygen. First, the photocatalytic reactivity of some photosensitizers [1,4-dicyanobenzene, 2,3,5,6-tetrafluoro-1,4-dicyanobenzene, and 9-phenylacridinium ion (AcrPh$^+$)] was examined for the photocatalytic oxygenation of 4,4′-dimethylbiphenyl to 4-(4′-methylphenyl)benzaldehyde in various solvents (eq 2).[22] Among the photosensitizers AcrPh$^+$ was the most effective photocatalyst in CDCl$_3$ (see the Supporting Information Figure S1 for the photocatalytic reactivity of the other photosensitizers).[23] The time course is shown in Figure 1, where the product yields were determined by ^{1}H NMR (see the Experimental Section).[24] 4-(4′-Methylphenyl)benzaldehyde is initially formed together with the small amounts of 4-(4′-methylphenyl)benzyl hydroperoxide and 4-(4′-methylphenyl)benzyl alcohol, accompanied by the disappearance of 4,4′-dimethylbiphenyl. The yield of 4-(4′-methylphenyl)benzyl hydroperoxide at 1 h photoirradiation was also determined as 4% by the iodometric titration (see the Experimental Section). The hydroperoxide disappeared after a prolonged irradiation time. This suggests that the hydroperoxide is an intermediate for the formation of 4-(4′-methylphenyl)benzaldehyde. It was confirmed that no corresponding carboxylic acid was formed during the photocatalytic reaction.[25]

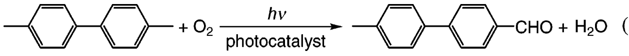

(2)

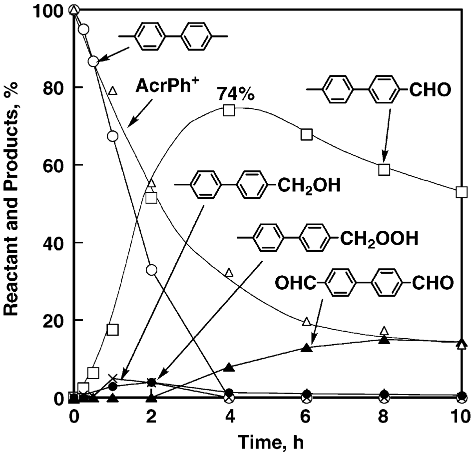

Figure 1. Time profiles of the disappearance of the reactant [4,4′-dimethylbiphenyl (○)] and formation of the products, 4-(4′-methlphenyl)benzaldehyde (□), 4,4′-diformylbiphenyl (▲), 4-(4′-methlphenyl)benzyl alcohol (×), and 4-(4′-methlphenyl)benzyl hydroperoxide (●), in the photocatalytic oxygenation of 4,4′-dimethylbiphenyl (3.0×10^{-2} M) in the presence of AcrPh$^+$ (4.0×10^{-3} M) in O$_2$-saturated CHCl$_3$ at 298 K. The amounts of the reactant and products are given as % in reference to the initial amount of 4,4′-dimethylbiphenyl.

The photocatalytic oxidation of 4-(4′-methylphenyl)benzyl alcohol to 4-(4′-methylphenyl)benzaldehyde with oxygen was independently examined, and it was found that the AcrPh$^+$-photocatalyzed oxidation of the alcohol proceeds more efficiently as compared with the photocatalytic oxygenation of 4,4′-dimethylbiphenyl (see the Supporting Information Figure S2).[26]

The monoaldehyde is further oxygenated to yield 4,4′-diformylbiphenyl after prolonged photoirradiation (Figure 1). After the photoirradiation for 4.0 h, the maximum yield of 4-(4′-methylphenyl)benzaldehyde is obtained (74%). Thus, AcrPh$^+$ acts as an efficient photocatalyst for the photoinduced oxygenation of 4,4′-dimethylbiphenyl with oxygen.

The AcrPh$^+$-photocatalytic oxygenation was also examined by using 4-(4′-methylphenyl)benzaldehyde as the starting material as shown in Figure 2, where 4-(4′-methylphenyl)benzaldehyde is further oxygenated with oxygen to yield 4,4′-diformylbiphenyl as the main oxygenated product.[24]

Photoinduced Electron Transfer from 4,4′-Dimethylbiphenyl to ^{1}AcrPh^{+*}. Irradiation of the absorption band of AcrPh$^+$ results in fluorescence at 508 nm in CHCl$_3$.[10] The fluorescence of the singlet excited state of AcrPh$^+$ (^{1}AcrPh^{+*}) is known to be quenched efficiently by a variety of aromatic electron donors via electron transfer from aromatic electron donors to ^{1}AcrPh^{+*}.[10] The quenching rate constants k_q were

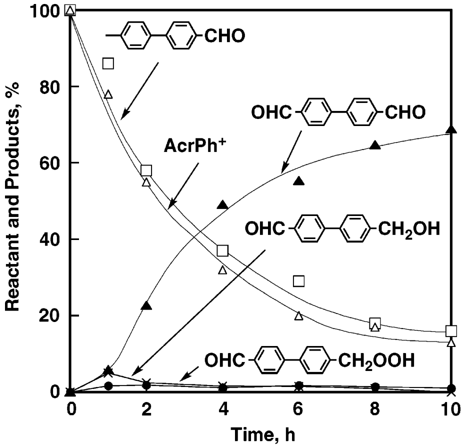

Figure 2. Time profiles of the disappearance of the reactant [4-(4′-methlphenyl)-benzaldehyde (□)] and formation of the products, 4,4′-diformylbiphenyl (▲) and 4-(4′-formylphenyl)benzyl alcohol (×), and 4-(4′-formylphenyl)benzyl hydroperoxide (●), in the photocatalytic oxygenation of 4-(4′-methlphenyl)benzaldehyde (3.0×10^{-2} M) in the presence of $AcrPh^+$ (4.0×10^{-3} M) in O_2-saturated $CHCl_3$ at 298 K. The amounts of the reactant and products are given as % in reference to the initial amount of 4-(4′-methlphenyl)benzaldehyde.

TABLE 1: Fluorescence Lifetimes (τ) of $ArcPh^+$, Fluorescence Quenching Rate Constants (k_q) of $AcrPh^+$ by 4,4′-Dimethylbiphenyl, One-Electron Reduction Potentials (E_{red}) of $AcrPh^+$, and One-Electron Reduction Potentials (E^*_{red}) of $^1AcrPh^{+*}$ in Various Solvents

solvent	τ, ns	k_q, M^{-1} s^{-1}	E_{red} vs SCE, V	E^*_{red} vs SCE, V
chloroform	2.6	1.1×10^{10}	−0.47	2.19
chlorobenzene	4.6	8.9×10^{9}	−0.45	2.20
dichloromethane	2.2	2.1×10^{10}	−0.49	2.17
tetrahydrofuran	1.6	1.7×10^{10}	−0.50	2.18
acetonitrile	1.4	2.2×10^{10}	−0.55	2.15

TABLE 2: One-Electron Oxidation Potentials (E_{ox}) of 4,4′-Dimethylbiphenyl, Free Energy Change (ΔG_{et}) of Electron Transfer from 4,4′-Dimethylbiphenyl to $^1AcrPh^{+*}$, and Limiting Quantum Yields (Φ_∞) of the Photocatalytic Oxygenation of 4,4′-Dimethylbiphenyl with Oxygen in Different Solvents

solvent	E_{ox} vs SCE, V	ΔG_{et}, eV	Φ_∞
chloroform	1.57	−0.62	0.12
chlorobenzene	1.56	−0.64	0.051
acetonitrile	1.54	−0.61	<0.01[a]

[a] Too small to be determined accurately.

determined from the slopes of the Stern−Volmer plots and the lifetime of the singlet excited state, $^1AcrPh^{+*}$ in different solvents (see the Supporting Information Figure S3). The k_q values thus obtained are summarized in Table 1.

The free energy change of photoinduced electron transfer from 4,4′-dimethylbiphenyl to $^1AcrPh^{+*}$ (ΔG_{et} in eV) is given by eq 3

$$\Delta G_{et} = e(E_{ox} - E^*_{red}) \tag{3}$$

where e is the elementary charge and E_{ox} and E^*_{red} are the one-electron oxidation potential of 4,4′-dimethylbiphenyl (1.57 V vs SCE in $CHCl_3$) and the one-electron reduction potential of $^1AcrPh^{+*}$ (2.19 V vs SCE in $CHCl_3$), respectively. Since the E_{ox} values of 4,4′-dimethylbiphenyl and E^*_{red} values of $AcrPh^{+*}$ in several solvents have been determined, the ΔG_{et} values are given from eq 3, as listed in Table 2. Judging from the exergonic nature of the photoinduced electron transfer ($\Delta G_{et} \ll 0$), the photoinduced electron transfer is expected to occur at the diffusion-limited rate,[27,28] and this is well verified experimentally (Table 1).

Detection of Radical Intermediates. The occurrence of photoinduced electron transfer from 4,4′-dimethylbiphenyl to $^1AcrPh^{+*}$ is confirmed by the laser flash photolysis experiments. Laser flash excitation (355 nm from an Nd:YAG laser) of an O_2-saturated $CHCl_3$ solution containing $AcrPh^+$ (5.6×10^{-5} M) and 4,4′-dimethylbiphenyl (1.0×10^{-1} M) affords a new transient absorption band at $\lambda_{max} = 690$ nm due to the radical cation of 4,4′-dimethylbiphenyl[29−31] and that at $\lambda_{max} = 520$ nm due to $AcrPh^\bullet$,[32] as shown in Figure 3a. Both absorption bands appear immediately after the nanosecond laser exposure.

Figure 4a shows the disappearance of absorbance at 690 nm in deaerated and O_2-saturated $CHCl_3$. The absorption band due to the radical cation of 4,4′-dimethylbiphenyl decays obeying first-order kinetics with the identical slope in the deaerated and O_2-saturated solution (Figure 4b), although the deviation from the linear plot is observed at the initial stage of the reaction due to the bimolecular back electron transfer from $AcrPh^\bullet$ to the radical cation.[33] Since benzyl radical is known to react with oxygen to give benzylperoxyl radical with the rate constant of $(2-4) \times 10^9$ M^{-1} s^{-1} in solution,[34] the lifetime of the benzyl radical in an O_2-saturated $CHCl_3$ solution ($[O_2] = 4.0 \times 10^{-2}$ M, see the Experimental Section) may be less than 0.1 μs. In such a case, the deprotonated benzyl type radical is not detected under the present experimental conditions.[35] From the linear plot of ln(ΔAbs at 690 nm) vs time in Figure 4b is obtained the deprotonation rate constant as 1.0×10^5 s^{-1}. This value is much smaller than the deprotonation rate constant of toluene radical cation in an aqueous solution (1.0×10^7 s^{-1}).[12a] The deprotonation rate constant is known to decrease with decreasing the ionization potential of the parent methylated benzene.[12,] Thus, the slower deprotonation rate from the radical cation of 4,4′-dimethylbiphenyl results from the lower one-electron oxidation potential than toluene.[10]

Laser flash excitation of $AcrPh^+$ in deaerated $CHCl_3$ solution containing 4,4′-dimethylbiphenyl affords virtually the same transient absorption bands (Figure 3b) as in the presence of oxygen (Figure 3a).

To detect the peroxyl radical produced by the reaction of the deprotonated benzyl type radical with oxygen, the ESR spectrum of an O_2-saturated CH_2Cl_2 solution containing $AcrPh^+$ (4.0×10^{-3} M) and 4,4′-dimethylbiphenyl (1.0×10^{-1} M) was measured under photoirradiation with a high-pressure mercury lamp at low temperature (see the Experimental Section). Figure 5 shows the detected ESR spectrum, which consists of two isotropic signals at $g = 2.0153$ and 2.0034. The former signal is readily assigned to 4-(4′-methylphenyl)benzylperoxyl radical because the g value is diagnostic of peroxyl radicals.[36,37] The latter signal is assigned to $AcrPh^\bullet$ by comparison with the reported ESR spectrum.[10]

Photocatalytic Oxygenation Mechanism. Based on the above results, the reaction mechanism for the $AcrPh^+$-photosensitized oxygenation of 4,4′-dimethylbiphenyl is summarized as shown in Scheme 1. Photoinduced electron transfer from 4,4′-dimethylbiphenyl (RH) to $^1AcrPh^{+*}$ occurs to produce the radical pair ($AcrPh^\bullet$ $RH^{\bullet+}$) as indicated by the efficient fluorescence quenching (Table 1). The geminate radical pair diffuses from the solvent cage to produce free radicals, $AcrPh^\bullet$ and $RH^{\bullet+}$, which were successfully detected as the transient absorption spectra in Figure 3. The deprotonation dynamics from $RH^{\bullet+}$ was directly monitored by the decay of absorbance at 690 nm due to $RH^{\bullet+}$ (Figure 4). The bimolecular back electron

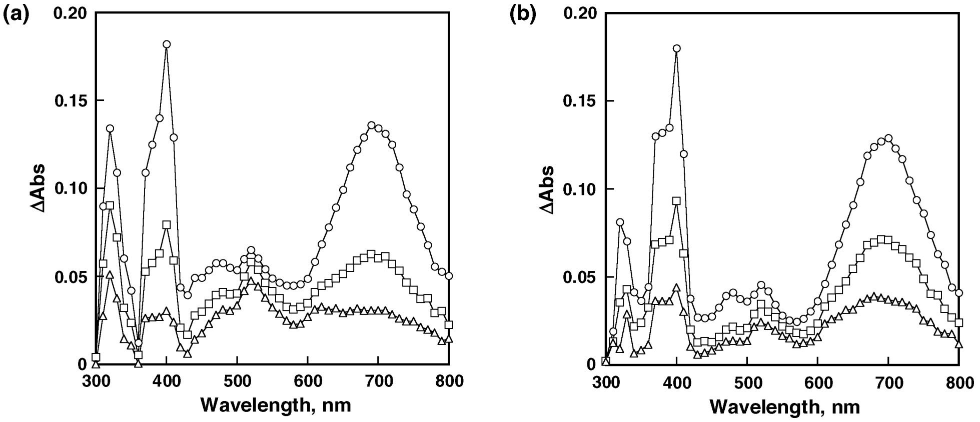

Figure 3. Transient absorption spectra observed by photoexcitation of (a) a deaerated and (b) an O_2-saturated $CHCl_3$ solution of $AcrPh^+$ (5.6×10^{-5} M) and 4,4′-dimethylbiphenyl (1.0×10^{-1} M) at 0.4 μs (○), 4.0 μs (□), and 10 μs (△) after laser excitation.

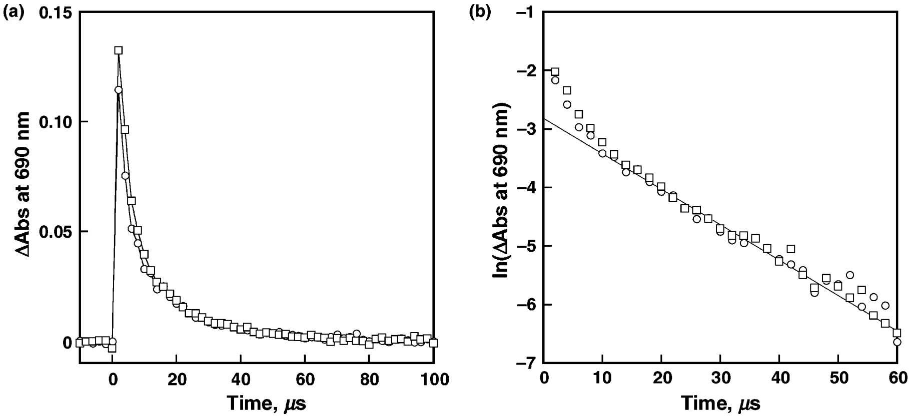

Figure 4. (a) Time dependence of absorbance at 690 nm observed by photoexcitation of a deaerated (○) and an O_2-saturated (□) $CHCl_3$ solution of $AcrPh^+$ (5.6×10^{-5} M) and 4,4′-dimethylbiphenyl (1.0×10^{-1} M) at 298 K. (b) First-order plot.

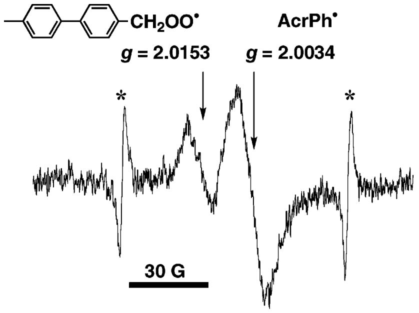

Figure 5. ESR spectrum observed under photoirradiation of an O_2-saturated dichloromethane solution of $AcrPh^+$ (4.0×10^{-3} M) containing 4,4′-dimethylbiphenyl (1.0×10^{-1} M) at 198 K. Asterisk denotes Mn^{2+} marker.

transfer from $AcrPh^\bullet$ to $RH^{\bullet+}$ (Scheme 1) also contributes to the decay of absorbance at 690 nm (Figure 4b). In the presence of oxygen, the deprotonated radical ($R^\bullet$) reacts with oxygen to produce the corresponding peroxyl radical, which is detected by ESR together with $AcrPh^\bullet$ in Figure 5. The bimolecular back electron transfer from $AcrPh^\bullet$ ($E_{red} = -0.47$ V vs SCE in $CHCl_3$)[32] to the peroxyl radical is exergonic,[38] thus occurring with the diffusion-limited rate to produce ROOH after protonation, accompanied by regeneration of $AcrPh^+$ (Scheme 1). This is confirmed by the second-order plot of the decay of the absorbance at 520 nm due to $AcrPh^\bullet$ in Figure 6. The second-order rate constant of back electron transfer is determined as 1.3×10^9 M^{-1} s^{-1} in $CHCl_3$ at 298 K.

The hydroperoxide decomposes to afford the corresponding aldehyde [4-(4′-methylphenyl)benzaldehyde] together with the corresponding alcohol [4-(4′-methylphenyl)benzyl alcohol] via radical chain decomposition of the hydroperoxide: the bimolecular reaction of $RO_2^\bullet$ gives two equiv of $RO^\bullet$ which abstracts hydrogen from ROOH to produce ROH, accompanied by regeneration of $RO_2^\bullet$ (Scheme 1). The alcohol is further oxidized via photoinduced electron transfer from the alcohol to $^1AcrPh^{+*}$ as reported for the photocatalytic oxidation of benzyl alcohol with $AcrH^+$ (see the Supporting Information Figure S2).[26,39]

SCHEME 1

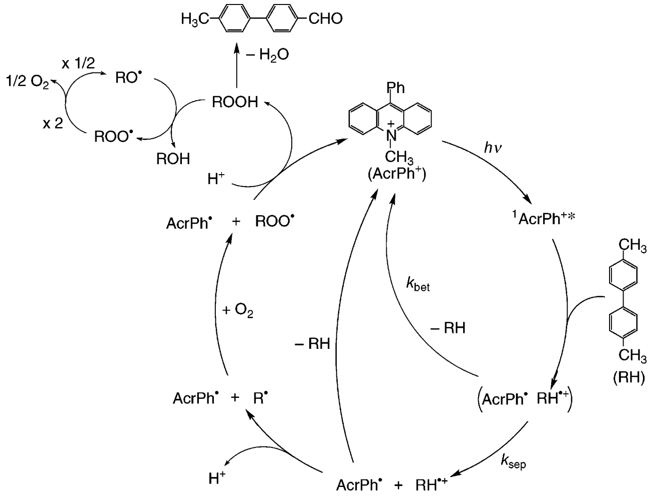

The photocatalytic cycle is repeated by starting with 4-(4′-methylphenyl)benzaldehyde instead of 4,4′-dimethylbiphenyl to yield 4,4′-diformylbiphenyl (Figure 2). Since the one-electron oxidation potential of the oxygenated product, 4-(4′-methylphenyl)benzaldehyde (1.76 V, vs SCE in $CHCl_3$), is still less

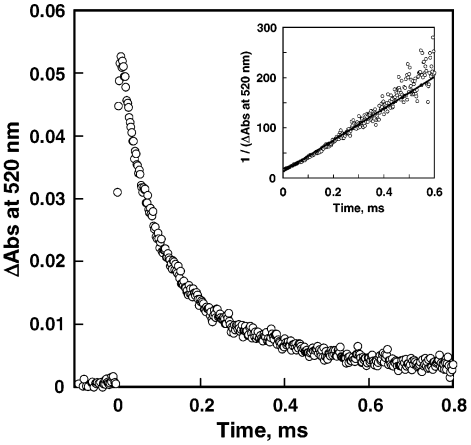

Figure 6. Decay time profile of absorbance at 520 nm observed by the photoexcitation of an O_2-saturated $CHCl_3$ solution of $AcrPh^+$ (5.6 $\times$ 10^{-5} M) and 4,4′-dimethylbiphenyl (0.10 M) at 298 K. Inset: Second-order plot.

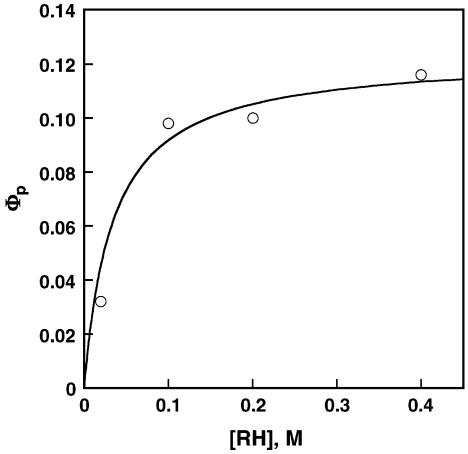

Figure 7. Dependence of the quantum yield (Φ_p) on concentration of 4,4′-dimethylbiphenyl [RH] for the $AcrPh^+$-catalyzed photooxygenation of 4,4′-dimethylbiphenyl in O_2-saturated $CHCl_3$ at 298 K.

positive than the one-electron reduction potential of $^1AcrH^{+*}$ (2.19 V vs SCE in $CHCl_3$, see Table 1), the further oxidation of 4-(4′-methylphenyl)benzaldehyde still occurs efficiently via photoinduced electron transfer from 4-(4′-methylphenyl)benzaldehyde to $^1AcrPh^{+*}$.

Quantum Yields of the Photocatalytic Oxygenation Reaction. The quantum yields (Φ_p) of the $AcrPh^+$-catalyzed photooxygenation of 4,4′-dimethylbiphenyl with oxygen in O_2-saturated $CHCl_3$ were determined from the formation rate of 4-(4′-dimethylbiphenyl)benzaldehyde under irradiation of monochromatized light of $\lambda = 430$ nm (see the Experimental Section). The Φ_p values increase with an increase in concentration of 4,4′-dimethylbiphenyl [RH] to reach a limiting value ($\Phi_p = 0.12$) as shown in Figure 7.

According to Scheme 1, the photocatalytic reaction proceeds via photoinduced electron transfer from RH to $^1AcrPh^{+*}$ to produce $RH^{\bullet+}$ and $AcrPh^\bullet$, when the dependence of Φ_p on [RH] is given by eq 4, and the limiting quantum yield (Φ_∞) is determined by the competition between the radical pair separation from the cage (k_{sep}) and the back electron transfer (k_{bet}) process as given by eq 5. The observed saturated

$$\Phi_p = \Phi_\infty k_{et}\tau[RH]/(1 + k_{et}\tau[RH]) \tag{4}$$

$$\Phi_\infty = k_{sep}/(k_{sep} + k_{bet}) \tag{5}$$

dependence of Φ_p on [RH] is well reproduced by eq 4 using the $k_q\tau$ value obtained from the fluorescence quenching of $^1AcrPh^{+*}$ by 4,4′-dimethylbiphenyl, as indicated by the solid line in Figure 7. This indicates that the photooxygenation of 4,4′-dimethylbiphenyl proceeds via the rate-limiting photoinduced electron transfer from 4,4′-dimethylbiphenyl to $^1AcrPh^{+*}$ and that no autoxidation process is involved in the photocatalytic oxygenation reaction.[40,41]

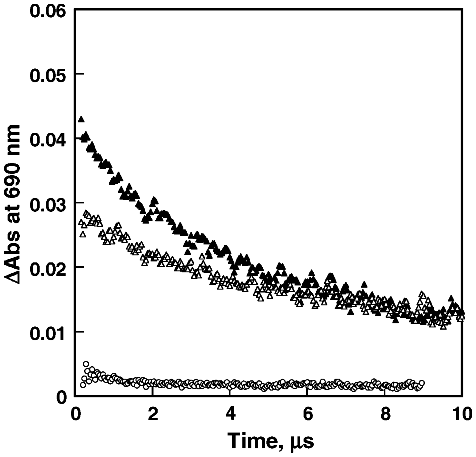

Figure 8. Decay time profiles of absorbance at 690 nm observed by photoexcitation of an O_2-saturated $CHCl_3$ (▲), C_6H_5Cl (△), and CH_3CN (○) solution of $AcrPh^+$ (5.6 $\times$ 10^{-5} M) and 4,4′-dimethylbiphenyl (1.0 $\times$ 10^{-1} M) at 298 K.

The Φ_∞ values were determined in different solvents as listed in Table 2. The Φ_∞ values are highly sensitive to the solvent polarity. The reason for such significant solvent effects is discussed below.

The Crucial Effects of Solvent. Photoinduced-electron-transfer reactions are normally performed in polar solvents (usually CH_3CN) because the solvation of the primary geminate radical-ion pairs facilitates the separation into free radical ions in solution.[28] However, the Φ_∞ value of the $AcrPh^+$-sensitized oxygenation reaction of 4,4′-dimethylbiphenyl decreases remarkably with increasing the solvent polarity: $\Phi_\infty = 0.12$ ($CHCl_3$), 0.05 (C_6H_5Cl), and 0 (CH_3CN) in Table 2.

According to eq 5, the large difference in the Φ_∞ value depending on the solvent polarity is determined mainly by the variation of the k_{bet} value of back electron transfer from $AcrPh^\bullet$ to $RH^{\bullet+}$ within the solvent cage, since the k_{sep} value of the separation of the geminate radical pair may be rather solvent independent.[29,32] The absorbance at 690 nm due to $RH^{\bullet+}$ detected immediately after nanosecond laser flash excitation (355 nm from an Nd:YAG laser) is compared in different solvents as shown in Figure 8. The detected concentration of $RH^{\bullet+}$ in different solvents decreases in the order $CHCl_3 > C_6H_5Cl \gg CH_3CN$, in agreement with the order of the Φ_∞ value in Table 2. Although the transient absorption band at 690 nm due to $RH^{\bullet+}$ is hardly detected in CH_3CN in the nanosecond laser flash photolysis measurements, it is clearly observed at 30 ps after the femtosecond laser excitation in CH_3CN as well as in $CHCl_3$ and C_6H_5Cl as shown in Figure 9a.[42] The absorbance at 690 nm due to $RH^{\bullet+}$ in CH_3CN decays rapidly due to the back electron transfer in the solvent cage as compared to the decay in $CHCl_3$ and C_6H_5Cl (Figure 9b).

Such drastic change in the back electron-transfer rate in the solvent cage depending on the solvent polarity is explained by the difference in the solvent reorganization energy of electron transfer (vide infra).

It has now been well established that the reorganization energy (λ) of electron transfer of charge-shift type of electron-

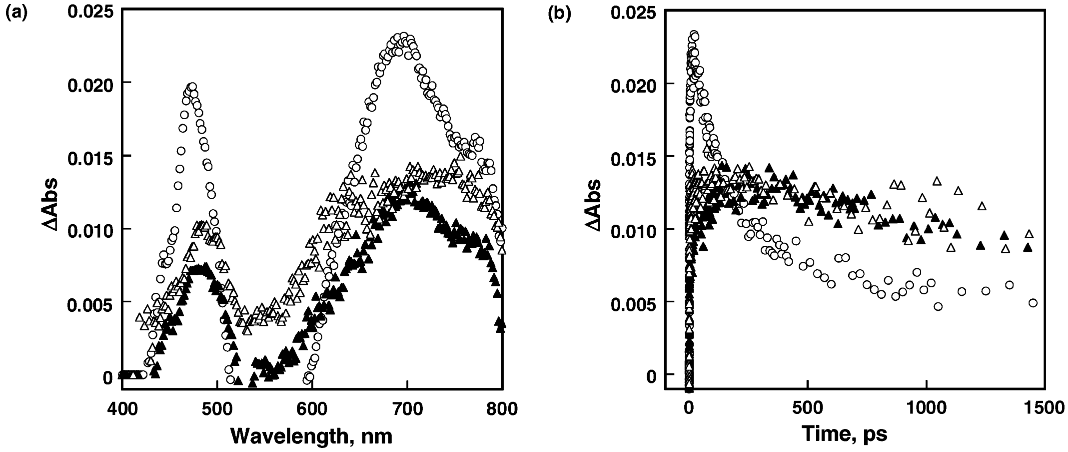

Figure 9. (a) Transient absorption spectra observed by photoexcitation of deaerated $CHCl_3$ (▲), C_6H_5Cl (△), and CH_3CN (○) solutions of $AcrPh^+$ (4.6×10^{-4} M) and 4,4′-dimethylbiphenyl (2.0×10^{-1} M) at 30 ps after the femtosecond laser excitation. (b) Time profiles of absorbance at 690 nm observed by photoexcitation of deaerated (○) $CHCl_3$ (▲), C_6H_5Cl (△), and CH_3CN (○) solutions of $AcrPh^+$ (4.6×10^{-4} M) and 4,4′-dimethylbiphenyl (2.0×10^{-1} M) at 298 K.

transfer such as from $AcrPh^\bullet$ to $RH^{\bullet+}$ decreases with decreasing the solvent polality.[29,32] On the other hand, the driving force of the charge-shift type of electron transfer is rather solvent independent.[32] In such a case, the rate of electron transfer from $AcrPh^\bullet$ to RH^+, which is deeply in the Marcus inverted region,[43,44] decreases with decreasing the solvent polarity, because the rate of electron transfer decreases with decreasing the reorganization energy of electron transfer in the Marcus inverted region.[32] Thus, the decrease in the back electron-transfer rate with decreasing the reorganization energy as the solvent polarity decreases results in the higher quantum yield of the formation of $RH^{\bullet+}$ and $AcrPh^\bullet$ in competition of the back electron transfer in the geminate radical pair, leading to the higher quantum yield of the oxygenated products.

Summary

The use of $AcrPh^+$ as a photocatalyst in $CHCl_3$ has enabled us to achieve highly selective photooxygenation of 4,4′-dimethylbiphenyl to 4-(4′-methylphenyl)benzaldehyde with molecular oxygen as an oxidant via photoinduced electron transfer from 4,4′-dimethylbiphenyl to $^1AcrPh^{+*}$ in $CHCl_3$. A further oxygenated product, 4,4′-diformylbiphenyl, was also obtained as a major product at prolonged irradiation time. The radical intermediates involved in the photocatalytic cycle were successfully detected as the transient absorption and the electron spin resonance spectra measurements. The high quantum yields of the oxygenated products in the $AcrPh^+$-photocatalyzed oxygenation of 4,4′-dimethylbiphenyl in $CHCl_3$ results from the slow back electron transfer from $AcrPh^\bullet$ to the radical cation of 4,4′-dimethylbiphenyl in the Marcus inverted region.

Acknowledgment. This work was partially supported by a Grant-in-Aid for Scientific Research Priority Area (Nos. 16205020 and 17750039) from the Ministry of Education, Culture, Sports, Science and Technology, Japan. One of the authors (K.S.) expresses his special thanks for the center of excellence (21COE) program “Creation of Integrated EcoChemistry of Osaka University”.

Supporting Information Available: Time profiles of the photocatalytic oxygenation of 4,4′-dimethylphenyl with oxygen using *p*-dicyanobenzene and tetrafluoro-*p*-dicyanobenzene (Figure S1), time profile of the $AcrPh^+$-catalyzed oxygenation of 4-(4′-methylphenyl)benzyl alcohol with oxygen (Figure S2), Stern−Volmer plots for the fluorescence quenching of $AcrPh^+$ by 4,4′-dimethylbiphenyl (Figure S3). This material is available free of charge via the Internet at http://pubs.acs.org.

References and Notes

(1) (a) Sheldon, R. A.; Kochi, J. K. In *Metal Catalyzed Oxidation of Organic Compounds*; Academic Press: New York, 1981; Chapter 10. (b) Franz, G.; Sheldon, R. A. In *Ullmann*’s *Encyclopedia of Industrial Chemistry*, 5th ed.; VCH: Weinheim, 1991. (c) Parshall, G. W.; Ittel, S. D. *Homogeneous Catalysis*, 2nd ed.; John Wiley & Sons: New York, 1992.

(2) (a) Anastas, P. T.; Warner, J. C. *Green Chemistry, Theory and Practice*; Oxford University Press: Oxford, U.K., 1998. (b) Clark, J. H. *Green Chem.* **1999**, *1*, 1. (c) Sheldon, R. A. *Green Chem.* **2000**, *2*, G1.

(3) (a) Trost, B. M. *Science* **1991**, *254*, 1471. (b) Dijksman, A.; Marino-Gonzalez, A.; Payeras, A. M. I.; Arends, I. W. C. E.; Sheldon, R. A. *J. Am. Chem. Soc.* **2001**, *123*, 6826. (c) Steinhoff, B. A.; Fix, S. R.; Stahl, S. S. *J. Am. Chem. Soc.* **2002**, *124*, 766. (d) Mori, K.; Hara, T.; Mizugaki, T.; Ebitani, K.; Kaneda, K. *J. Am. Chem. Soc.* **2004**, *126*, 10657.

(4) Oelgemoeller, M.; Jung, C.; Ortner, J.; Mattay, J.; Zimmermann, E. *Green Chem.* **2005**, *7*, 35.

(5) An, B.-K.; Kwon, S.-K.; Jung, S.-D.; Park, S. Y. *J. Am. Chem. Soc.* **2002**, *124*, 14410.

(6) Williams, V. E.; Lemieux, R. P. *J. Am. Chem. Soc.* **1998**, *120*, 11311.

(7) Bolognesi, M. L.; Bixel, M. G.; Marucci, G.; Bartolini, M.; Krauss, M.; Angeli, P.; Antonello, A.; Rosini, M.; Tumiatti, V.; Hucho, F.; Melchiorre, C. *J. Med. Chem.* **2002**, *45*, 3286.

(8) Helms, A.; Heiler, D.; McLendon, G. *J. Am. Chem. Soc.* **1992**, *114*, 6227.

(9) ,4′-Diformylbiphenyl was also prepared by the Suzuki coupling reaction of 4-formylboronic acid with 4-bromobenzaldehyde, see: (a) Kuroboshi, M.; Waki, Y.; Tanaka, H. *J. Org. Chem.* **2003**, *68*, 3938. (b) Moutloali, R. M.; Nevondo, F. A.; Darkwa, J.; Iwuoha, E. I.; Henderson, W. *J. Organomet. Chem.* **2002**, *656*, 262.

(10) (a) Ohkubo, K.; Suga, K.; Morikawa, K.; Fukuzumi, S. *J. Am. Chem. Soc.* **2003**, *125*, 12850. (b) Ohkubo, K.; Fukuzumi, S. *Org. Lett.* **2000**, *2*, 3647.

(11) Bietti, M.; Steenken, S. In *Electron Transfer in Chemistry*; Balzani, V., Ed.; Wiley-VCH: Weinheim, 2001; Vol. 2, pp 494−579.

(12) For deprotonation rates in H_2O, see: (a) Sehested, K.; Holcman, J. *J. Phys. Chem.* **1978**, *82*, 651. (b) Russo-Caia, C.; Steenken, S. *Phys. Chem. Chem. Phys.* **2002**, *4*, 1478.

(13) Armarego, W. L. F.; Perrin, D. D. *Purification of Laboratory Chemicals,* 4th ed.; Butterworth-Heinemann: Oxford, 1996.

(14) Hatchard, C. G.; Parker, C. A. *Proc. R. Soc. London, Ser. A* **1956**, *235*, 518.

(15) Fukuzumi, S.; Ohkubo, K.; Tokuda, Y.; Suenobu, T. *J. Am. Chem. Soc.* **2000**, *122*, 4286.

(16) Fukuzumi, S.; Koumitsu, S.; Hironaka, K.; Tanaka, T. *J. Am. Chem. Soc.* **1987**, *109*, 305.

(17) Fukuzumi, S.; Kuroda, S.; Tanaka, T. *J. Am. Chem. Soc.* **1985**, *107*, 3020.

(18) Mair, R. D.; Graupner, A. J. *Anal. Chem.* **1964**, *36*, 194.

(19) Fukuzumi, S.; Ishikawa, M.; Tanaka, T. *J. Chem. Soc., Perkin Trans. 2* **1989**, 1037.

(20) The SHACV method provides a superior approach to directly evaluating the one-electron redox potentials in the presence of a follow-up chemical reaction, relative to the better-known dc and fundamental harmonic ac methods, see: (a) Bond, A. M.; Smith, D. E. *Anal. Chem.* **1974**, *46*, 1946. (b) Arnett, E. M.; Amarnath, K.; Harvey, N. G.; Cheng, J.-P. *J. Am. Chem. Soc.* **1990**, *112*, 344.

(21) Mann, C. K.; Barnes, K. K. *Electrochemical Reactions in Nonaqueous Systems*; Mercel Dekker: New York, 1970.

(22) AcrPh$^+$ was not soluble in nonpolar solvents such as benzene and hexane. Chloroform was the best solvent to afford the largest quantum yield among examined solvents in which AcrPh$^+$ was soluble (chloroform, chlorobenzene, dichloromethane, tetrahydrofuran, and acetonitrile).

(23) The photocatalytic oxygenation reaction of 4,4′-dimethylbiphenyl has hardly occurred in CH$_3$CN (the yield $<$ 1% after 12 h photoirradiation).

(24) Although the concentration of AcrPh$^+$ decreases with photoirradiation time, AcrPh$^+$ still remains after 10 h photoirradiation, acting as an effective photocatalyst (Figures 1 and 2).

(25) Some precipitates were formed at a prolonged irradiation time, indicating the formation of small amounts of polymeric products.

(26) For the AcrH$^+$-photocatalyzed oxidation of benzyl alcohol with oxygen, see: Fukuzumi, S.; Kuroda, S.; Tanaka, T. *J. Chem. Soc., Chem. Commun*. **1987**, 120.

(27) (a) Rehm, D.; Weller, A. *Ber. Bunsen-Ges. Phys. Chem.* **1969**, *73*, 834. (b) Rehm, D.; Weller, A. *Isr. J. Chem*. **1970**, *8*, 259.

(28) Kavarnos, G. J. In *Fundamental of Photoinduced Electron Transfer*; Wiley-VCH: New York, 1993.

(29) Gould, I. R.; Ege, D.; Moser J. E.; Farid, S. *J. Am. Chem. Soc*. **1990**, *112*, 4290.

(30) Dileesh, S.; Gopidas, K. R. *Chem. Phys. Lett*. **2000**, *330*, 397.

(31) No triplet−triplet absorption due to 4,4′-dimethylbiphenyl was observed under the present experimental conditions. For the triplet−triplet absorption due to 4,4′-dimethylbiphenyl and biphenyl, see: (a) Naik, D. B.; Dey, G. R.; Kishore, K.; Moorthy, P. N. *J. Photochem. Photobiol., A* **1992**, *68*, 337. (b) Cai, X.; Sakamoto, M.; Hara, M.; Tojo, S.; Kawai, K.; Endo, M.; Fujitsuka, M.; Majima, T. *J. Phys. Chem. A* **2004**, *108*, 9361.

(32) Fukuzumi, S.; Ohkubo, K.; Suenobu, T.; Kato, K.; Fujitsuka, M.; Ito, O. *J. Am. Chem. Soc*. **2001**, *123*, 8459.

(33) Although the decay of the radical cation of 4,4′-dimethylbiphenyl in deaerated solution looks faster than that in O$_2$-saturated solution at the initial state of the reaction (Figure 3), the overall decay time profiles in the absence and presence of oxygen including the prolonged reaction time (Figure 4a) are virtually the same. The bimolecular back electron transfer from AcrPh$^\bullet$ to the radical cation in the absence of oxygen contributes to the second-order decay of the absorbance at 690 nm at the initial stage of the reaction in addition to the first-order decay due to the deprotonation of the radical cation, whereas AcrPh$^\bullet$ is partially quenched by oxygen in the O$_2$-saturated solution to retard the bimolecular back electron transfer from AcrPh$^\bullet$ to the radical cation. This may be the reason the decay of the radical cation in the absence of oxygen is faster than that in the presence of oxygen at the initial stage of the reaction (Figure 3).

(34) (a) Maillard, B.; Ingold, K. U.; Scaiano, J. C. *J. Am. Chem. Soc.* **1983**, *105*, 5095. (b) Tokumura, K.; Ozaki, T.; Nosaka, H.; Saigusa, Y.; Ito, M. *J. Am. Chem. Soc.* **1991**, *113*, 4974. (c) Tokumura, K.; Nosaka, H.; Ozaki, T. *Chem. Phys. Lett*. **1990**, *169*, 321.

(35) The absorption bands due to the benzyl type radical appear at $\lambda =$ 320 nm, see: (a) Porter, G.; Wright, F. J. *Trans. Faraday Soc*. **1955**, *51*, 1469. (b) Tokumura, K.; Ozaki, T.; Nosaka, H.; Saigusa, Y.; Itoh, M. *J. Am. Chem. Soc.* **1991**, *113*, 4974. The present experimental conditions in the presence of a large concentration of 4,4′-dimethylbiphenyl have also precluded the detection of the benzyl type radical.

(36) (a) Bally, T.; Roth, K.; Straub, R. *J. Am. Chem. Soc.* **1988**, *110*, 1639. (b) Badger, B.; Brocklehurst, B. *Trans. Faraday Soc.* **1969**, *65*, 2582 and 2588. (c) Gerson, F.; Kaupp, G.; Ohya-Nishiguchi, O. *Angew. Chem., Int. Ed. Engl.* **1977**, *16*, 657. (d) Badger, B.; Brocklehurst, B. *Trans. Faraday Soc.* **1970**, *66*, 2939. (e) Rodgers, M. A. J. *J. Chem. Soc., Faraday Trans. 1* **1972**, *68*, 1278. (f) Inokuchi, Y.; Naitoh, Y.; Ohashi, K.; Saitow, K.-I.; Yoshihara, K.; Nishi, N. *Chem. Phys. Lett.* **1997**, *269*, 298.

(37) Cumylperoxyl radical has been reported as $g = 2.0156$: (a) Bersohn, M.; Thomas, J. R. *J. Am. Chem.* Soc. **1964**, *86*, 959. (b) Fukuzumi, S.; Ono, Y. *J. Chem. Soc., Perkin Trans. 2* **1977**, 622.

(38) The one-electron reduction potential of RO$_2^\bullet$ was determined as 0.67 V which is much more positive than the oxidation potential of AcrPh$^\bullet$ ($-$0.47 V vs SCE in CHCl$_3$),[32] see: Fukuzumi, S.; Shimoosako, K.; Suenobu, T.; Watanabe, Y. *J. Am. Chem. Soc*. **2003**, *125*, 9074.

(39) Fukuzumi, S.; Tanaka, T. *Photoinduced Electron Transfer*; Fox, M. A., Chanon, M., Ed.; Elsevier: Amsterdam, 1988; Part C, p 578.

(40) If the autoxidation process plays an important role in the photocatalytic oxygenation of RH, the quantum yield would increase linearly with increasing RH concentration, see: Suga, K.; Ohkubo, K.; Fukuzumi, S. *J. Phys. Chem. A* **2003**, *107*, 4339. For autoxidation processes initiated by photoinduced electron transfer, see: Saito, I.; Tamoto, K.; Matsuura, T. *Tetrahedron Lett*. **1979**, 2889.

(41) In contrast to the case of laser-flash photolysis experiments (Figure 4), the contribution of the bimolecular back electron transfer is negligible under the steady-state photoirradiation for the determination of the quantum yield (Figure 7), when the concentrations of AcrPh$^\bullet$ and RH$^{\bullet+}$ are much smaller than those in Figure 4.

(42) The transient absorption band at 520 nm due to AcrPh$^\bullet$ observed in Figure 3 is masked by the emission of ^{1}AcrPh^{+*} in Figure 9a.

(43) (a) Marcus, R. A. *Annu. Rev. Phys. Chem*. **1964**, *15*, 155. (b) Marcus, R. A. *Angew. Chem., Int. Ed. Engl.* **1993**, *32*, 1111.

(44) For the Marcus inverted region, see: (a) Miller, J. R.; Calcaterra, L. T.; Closs, G. L. *J. Am. Chem. Soc.* **1984**, *106*, 3047. (b) Closs, G. L.; Miller, J. R. *Science* **1988**, *240*, 440. (c) Gould, I. R.; Farid, S. *Acc. Chem. Res.* **1996**, *29*, 522. (d) McLendon, G. *Acc. Chem. Res.* **1988**, *21*, 160. (e) Winkler, J. R.; Gray, H. B. *Chem. Rev.* **1992**, *92*, 369. (f) McLendon, G.; Hake, R. *Chem. Rev.* **1992**, *92*, 481.